# Reactions Between Melamine Formaldehyde Resin and Cellulose: Influence of pH

C. DEVALLENCOURT,[1] J. M. SAITER,[1] D. CAPITAINE[2]

[1] Laboratoire d'Etude et de Caractérisation des Amorphes et des Polymères, Departement des Sciences, Université de Rouen, 76821 Mont Saint-Aignan Cédex, France

[2] OFITECH S.A., Z.I., B.P. 17, 76480 Yainville, France

*Received 9 March 1998; accepted 15 November 1999*

**ABSTRACT:** Nuclear magnetic resonance of $^{13}C$ in the liquid state and dynamic mechanical analysis were performed on composite materials obtained from a sample of ashless filter paper immersed in aqueous solutions of a melamine formaldehyde resin with a high NH ratio. The resin aqueous solution was studied at pH 6, 7, and 9. After a cure performed at 85°C we showed that acid conditions improved the mechanical properties of the composite because of self-condensation reactions of the amino resin while for the other pH values the mechanical properties of the cellulose were not changed because mainly hydrolysis reactions occurred. For a cure performed at 140°C and under acid conditions the degree of crosslinking of the resin increased while for the other pH mainly cocondensation reactions appeared. Finally, from the study of moisture sorption measurements performed on a composite material elaborated at pH 7 and for different relative humidity values we showed that mainly the Langmuir absorption mode was modified by the presence of the resin. This last result allowed us to propose a complete scenario of the events that appeared during the formation of the composite material. © 2000 John Wiley & Sons, Inc. J Appl Polym Sci 78: 1884–1896, 2000

**Key words:** melamine formaldehyde resin; cellulose; composite; mechanical properties; pH; self-condensation reaction; cocondensation reaction

## INTRODUCTION

Melamine formaldehyde resins are incorporated in many coating formulations to improve the mechanical properties or the resistance to humidity or to modify the adhesion of other materials.[1] They can also be used in the same field as curing elements for other resins or as fire retardants.[2] The basic melamine structure consists of an aromatic triazine ring with six substituent sites, two on each terminal nitrogen (see Fig. 1). When convenient conditions of cure are performed, the melamine formaldehyde resins mixed with a polyol as a cellulose lead to the formation of a composite material. The nature of the chemical reactions concerning the self-condensation reactions of the resin and the cocondensation reactions of the resin with a polyol are difficult to study, because as noted by Jones et al.,[3,4] both components are complex systems, a variety of different reactions can occur, the water action is of prime importance, and most of the reactions are reversible. In spite of this complexity, the crosslinking reactions of melamine formaldehyde resins were extensively studied by Blank and coworkers.[5–8] These

*Correspondence to:* J. M. Saiter.

Contract grant sponsor: Haute Normandie Region; contract grant number: 3006-674-R3.

Journal of Applied Polymer Science, Vol. 78, 1884–1896 (2000)

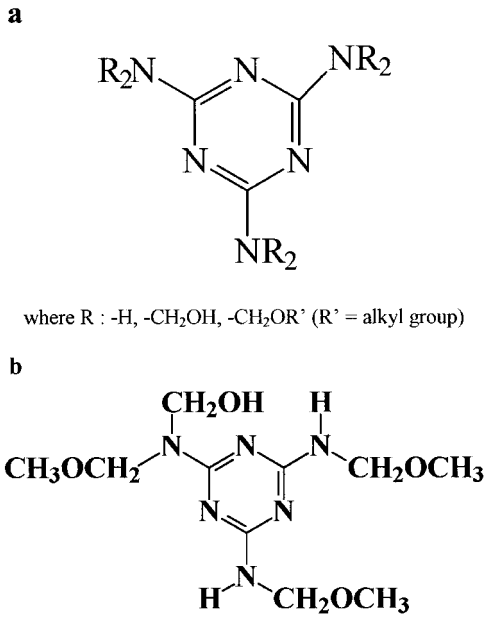


**Figure 1** (a) The chemical structure of a melamine formaldehyde resin and (b) an example of an highly methylated, high —NH melamine formaldehyde resin with these reactive sites.

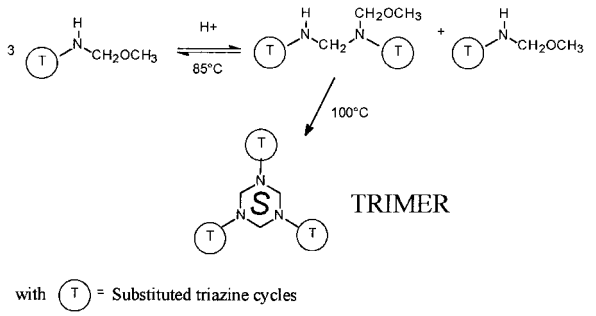


**Figure 2** The potential reaction mechanism to form cyclic methylene bridges in amino compounds.

authors showed that the difference in cure mechanisms among fully alkylated, partially alkylated, and highly alkylated melamine formaldehyde resins with a high —NH ratio had significant implications from a formulation standpoint. They cataloged 11 reactions (Table I) that led to volatile by-products,[7] which could describe what is expected for a highly methylated resin with a high —NH ratio. The sites responsive to general acid catalysis or a weak undissociated acid on a melamine formaldehyde resin are mainly the —$NHCH_2OCH_3$ groups or the —$NCH_2OH(CH_2OCH_3)$ functionality that can demethylolate in a melamine formaldehyde resin and forms the —$NHCH_2OCH_3$ group (reaction 1 in Table I). The self-condensation reactions of amino resins during the manufacturing process produces either methylene (reactions 2, 5) or methylene ether bridges (reactions 6, 7) between the amino compounds. In melamine resins the methylene group is favored if a lower formaldehyde charge is used in processing, but this reaction is readily reversible and the bridges are unstable.[4] Jones et al.[3] and Bauer[9] go up to the point that transient acyclic methylene bridges can, through a sequence of reversible reactions, form cyclic methylene bridge structures exemplified by the trimer presented in Figure 2. Formation of cyclic bridges exhibits a slower kinetic than formation of acyclic bridges, but when formed they are stable. In table I, we note that reaction 3 is observed only at high tem-

**Table I Self-Condensation and Cocondensation Reactions for Highly Methylated, High —NH Melamine Formaldehyde Resin with Polyol**

| Reaction No. | Reaction |
|---|---|
| 1 | —$NCH_2OH \rightarrow$ —$NH + H_2C{=}O$ |
| 2 | —$NCH_2OCH_3$ + —$NH \rightarrow$ —$NCH_2N$— + $CH_3OH$ |
| 3 | 2-$NCH_2OCH_3 \rightarrow$ —$NCH_2N$— + $CH_3OCH_2OCH_3$ |
| 4 | —$NCH_2OH$ + —$NH \rightarrow$ —$NCH_2N$— + $H_2O$ |
| 5 | 2-$NCH_2OH \rightarrow$ —$NCH_2N$— + $H_2C{=}O + H_2O$ |
| 6 | —$NCH_2OCH_3$ + —$NCH_2OH \rightarrow$ —$NCH_2OCH_2N$— + $CH_3OH$ |
| 7 | 2-$NCH_2OH \rightarrow$ —$NCH_2OCH_2N$— + $H_2O$ |
| 8 | 2-$NCH_2OCH_3 + H_2O \rightarrow$ —$NCH_2N$— ++ $2CH_3OH$ |
| 9 | —$NCH_2OCH_3 + H_2O \rightarrow$ —$NCH_2OH + CH_3OH$ |
| 10 | —$NCH_2OCH_3$ + R′OH → —$NCH_2OR' + CH_3OH$ |
| 11 | —$NCH_2OH$ + R′OH → —$NCH_2OR' + H_2O$ |

R′, an alkyl group.

peratures.[10] Reactions 8 and 9 are obtained under very humid conditions. Finally, by mixing with a polyol, two further cocondensation reactions between the resin and the polyol can occur[5] (reactions 10 and 11, Table I).

Although in many studied systems the composite is obtained by dissolving the resin and the polyol in an aqueous solution and thus the reactions take place from dilute systems, in this work the cellulose that acted as the polyol was not dissolved but remained in the solid state and was only immersed in the aqueous resin solution. The aqueous resin solutions were studied at pH 6, 7, and 9 and two curing temperatures of 85 and 140°C. The mechanical properties of the materials obtained after these different treatments were analyzed, as were the effects on the moisture absorption.

## EXPERIMENTAL

### Materials

The melamine resin used in this work (Urecoll MK resin, BASF) was analyzed in a previous work by thermogravimetry and Fourier transform IR coupling investigations.[11] We determined the combined molar ratio of melamine formaldehyde and methane alcohol as $MF_{\geq 4.4}$ and $Me_{4.4}$, respectively. Methane alcohol was combined in the form of methoxymethyl groups ($>NCH_2OCH_3$). The cellulose sample used in this work was an ashless number 111 paper supplied by Durieux. The thermogravimetric measurements showed that this cellulose is characteristic of a chemical paper pulp product with a high degree of crystallinity (>80%).[12] This cellulose was found to be chemically stable for temperatures up to 280°C under a nitrogen atmosphere.[13]

The dilution rate of the commercial resin is about 37% by weight. Three pH values for the aqueous resin solution were studied: the first one was a resin with a buffer solution of isophthalate/isophthalic acid (pH 6), the second one was an aqueous resin solution (pH 7), and the third one was a resin with a buffer solution of borate/boric acid (pH 9). Samples obtained with these three experimental conditions were called a, b, and c, respectively. The duration of the immersion was chosen in such a way that the absorption reached its maximum. Then the sample was taken out of the bath, wiped, and cured in an oven. Two curing temperatures ($T_c$) were used: 85 and 140°C.

For the spectrometry analysis by $^{13}$C-NMR, the samples after the cure period were washed with hot water (100°C) and then dissolved in a lithium chloride/*N*,*N*-dimethylacetamide (LiCl/DMAc) solvent system as described in detail by Mc Cormick et al.[14]

### Nuclear Magnetic Resonance

All $^{13}$C-NMR spectra were measured with a Bruker ARX 400 spectrometer. The spectrometer had a C probe system operating at 22.5 MHz for $^{13}$C. The tube size was 10 mm (large band). The spin-lattice relaxation time (10 s) was determined through an inversion recovery technique with an exponential fit to look for the relaxation of carbons in triazine cycles. Dimethyl sulfoxide was used as a standard. Each sample studied was submitted to the magnetic field for 19 h and two temperatures were checked (20 and 70°C). Finally, composite solutions were prepared by suspending composite materials or cellulose (~ 5% w/v) in LiCl/DMAc 8% (w/w).

### Dynamic Mechanical Analysis

Viscoelastic analysis was carried out using a Metravib instrument. Parallelepipedic samples (15 × 20 × 0.2 mm) were clamped in the jaws of the instrument, placed under sufficient tension to avoid flapping, and exposed to an oscillating tensile deformation at a frequency of 5 Hz. The definitions of dynamic properties are given in Figure 3 in terms of maximum oscillatory stress ($\varepsilon_0$), the maximum resulting strain ($\sigma_0$), and the phase lag ($\delta$). Data output included storage modulus ($E'$), loss modulus ($E''$), and loss tangent (tan $\delta$). These dynamic properties were determined at 1°C intervals. The −100 to 250°C temperature range was scanned with a heating rate of 5°C/min under an air atmosphere.

### Moisture Sorption

Experimental measurements were performed on composite material made from recycled cellulose and a resin solution at pH 7 (actually $2.87 \pm 0.05$ $10^{-2}$ cm thick). This recycled cellulose, called sample e, contains a weight ratio of 70/30 for the mechanical/chemical paper pulps with a filler content of about 15.44%. The composite material made this way is called sample f. The cure temperature of 100°C was held for 3 h (More details about the manufacturing of recycled cellulose can be found in our previous work.[13] For the gravim-

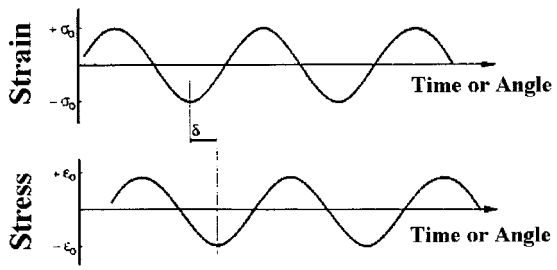


| | |
|---|---|
| **Storage modulus** | $E' = \frac{\sigma_0 \cos\delta}{\varepsilon_0}$ |
| **Loss modulus** | $E'' = \frac{\sigma_0 \sin\delta}{\varepsilon_0}$ |
| **Loss tangent** | $\frac{E''}{E'} = \tan\delta$ |

**Figure 3** Plots showing oscillating strain and stress and equations that define dynamic properties. Maximum values of strain ($\varepsilon_0$) and stress ($\sigma_0$) are indicated.

etry study the original plate was cut into parallelepipedic samples (8 × 4 cm). Dry specimens were obtained by drying them in a vacuum dessicator in the presence of $P_2O_5$ until constant weight. Humidity conditioning was achieved by storing samples at room temperature (25 ± 1°C) in dessicators with relative humidities (RHs) adjusted to 25, 73, and 95% by using aqueous sulfuric acid solutions at different concentrations (55, 30, and 10% w/w of $H_2SO_4$, respectively). These humidity conditions were controlled by a TTH.20 Snelco moisture/temperature sensor that has a known accuracy of about 2%.

In the water sorption kinetic experiments the dry samples were introduced in the dessicators or in water, periodically removed, and weighed using an AE 240 Mettler analytical balance with an accuracy of 0.01 mg. The samples were considered as at moisture equilibrium when the moisture regain remained constant.

## RESULTS

Figures 4–6 present the $^{13}$C-NMR spectra in LiCl/DMAc solvent performed on our cellulose and on samples b and c after a cure at 85°C. The chemical shifts and their assignments are given in Table II. Note that no spectra are presented for sample a cured at 85°C and for samples a, b, and c cured at 140°C. Indeed, we found that these last samples exhibited a high level of resistance to all the solvents tested in this work.

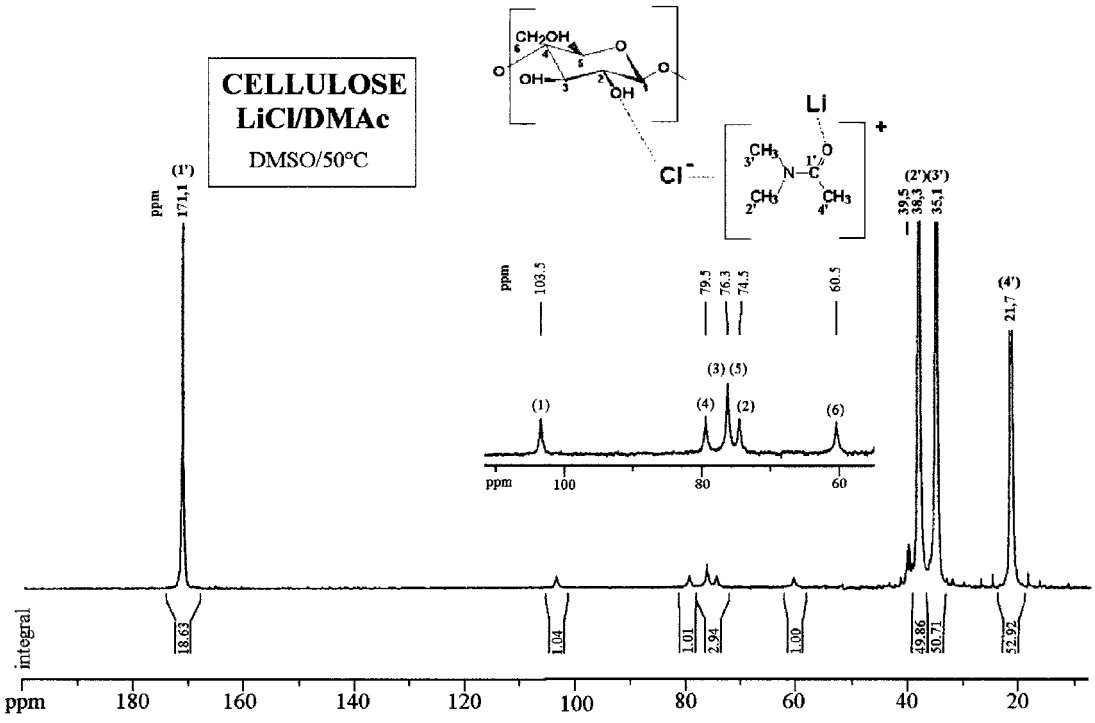


**Figure 4** Proton decoupled $^{13}$C-NMR spectra of a 5% (w/w) solution of a pure cellulose (sample d) in an 8% LiCl/DMAc solvent system and recorded at 70°C.

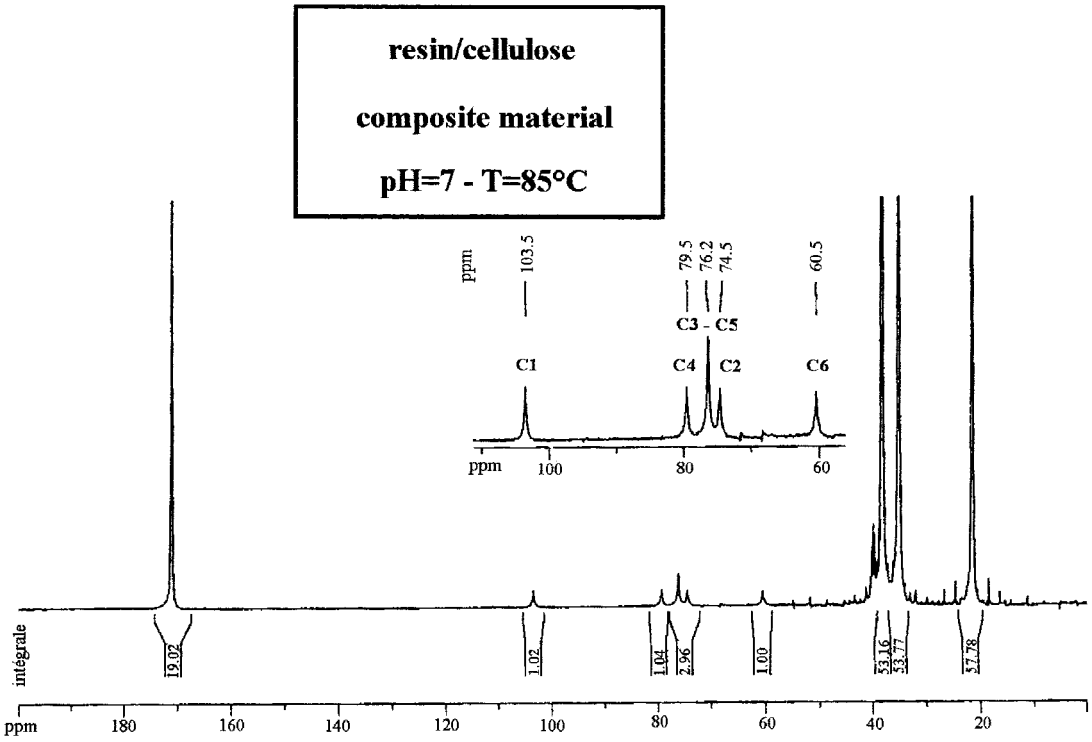


**Figure 5** Proton decoupled $^{13}$C-NMR spectra of a 5% (w/w) solution of composite material in 8% LiCl/DMAc made from a resin solution at pH 7 and recorded at 70°C (sample b).

Figure 4 contains the proton decoupled $^{13}$C-NMR spectra of a 5% cellulose solution in 8% LiCl/DMAc at 70°C. First of all we observe the major resonance of four signals that identify the LiCl/DMAc solvent system. The $C_1'$ carbon, the most deshielded, is assigned to the peak at 171 ppm. Carbons $C_2'$–$C_4'$ are assigned in the opposite direction: the signals of $C_2'$ [$\underline{C}H_3$—(N—) group], $C_3'$, and $C_4'$ [$\underline{C}H_2$—CO(N—) group] are at 38, 35, and 22 ppm, respectively. Then five minor peaks between 50 and 110 ppm are readily identified for the cellulose. The five cellulose peaks can be assigned by comparing them with other cellulose solutions[15] and to solid-state spectra[15] and their apparent sharpness indicates that the LiCl/DMAc solution is indeed a real solvent system for cellulose. The $C_1$ carbon, the most deshielded, is assigned to the peak at 103.5 ppm. The other easily assignable peak is the $C_6$ carbon at 60.5 ppm. The three interior peaks from the low to high field (79.5, 76.3, and 74.5 ppm) are assigned to the $C_4$, the $C_3$ and $C_5$ overlap, and the $C_2$ carbon, respectively.

Figure 5 shows the proton decoupled $^{13}$C-NMR spectra obtained on sample b ($T_c$ = 85°C, pH 7). Note that no difference appears between the spectra presented in Figures 4 and 5. In other words, this indicates that after being washed in water no resin remains in this sample.

Figure 6 shows the proton decoupled $^{13}$C-NMR spectra obtained on sample c ($T_c$ = 85°C, pH 9). No main difference appears between this spectra and the previous one, except for some peaks of small magnitude in the range of 160–170 ppm. Thus, as for sample b, practically no resin remains in this sample after being washed in water.

The viscoelastic measurements led to the determination of the storage modulus values ($E'$) and tan $\delta$ values for each temperature scanned during the heating program. Thus, for each curing temperature two curves were recorded: $E' = f(T)$ and tan $\delta = f(T)$. The results obtained for the cellulose (sample d) and samples a, b, and c and for the two temperatures of cure (85 and 140°C) are reported in Figures 7–10.

For a $T_c$ of 85°C, we observe the same variations of the storage modulus versus the temperature (Fig. 7) for the cellulosic sample (sample d) and samples b and c. Indeed, at low temperatures and up to 100°C, the value of the storage modulus

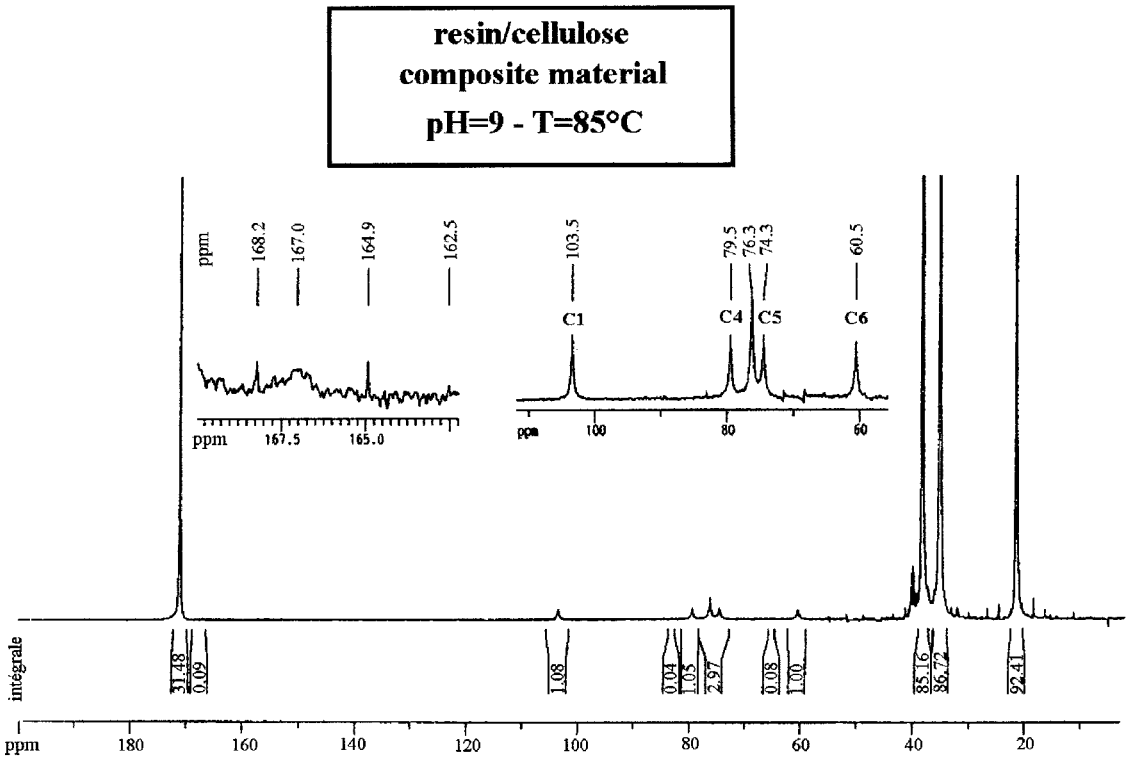


**Figure 6** Proton decoupled $^{13}$C-NMR spectra of a 5% (w/w) solution of composite material in 8% LiCl/DMAc made from a resin solution at pH 9 and recorded at 70°C (sample c).

decreases slowly with the temperature; and for the temperature range between 100 and 200°C, the values of the storage modulus fall roughly from $2 \times 10^9$–$10^7$ N m$^{-2}$. For sample a this variation is observed as a double step phenomenon, and it appears between 130 and 220°C. Finally, for high temperatures (>200°C) a new regime with a small decreasing of $E'$ is observed except for sample a. For the same curing temperature all the associated tan $\delta = f(T)$ curves (Fig. 8) exhibit a peak of low magnitude at a low temperature (−55°C). This peak is due to local motions located along the polymeric chains of the cellulose and corresponds to the $\beta$ relaxation.[16–19] This relaxation is noncooperative. In the range of temperatures located around the large decrease of the storage modulus, the tan $\delta = f(T)$ curves show a peak of large magnitude, except for sample a. This peak occurs in a range of temperatures lower than those expected for the degradation process that, as shown by Dollimore and Hoath[20] and in one of our previous works,[13] occurs at > 250°C, which is independent of the gas flow nature (air, nitrogen). On the other hand, the amorphous part of a cellulose can be separated into two large species: the first one is a domain that exhibits strong intra- and intermolecular hydrogen bounds; the second one exhibits weak intra- and intermolecular hydrogen bonds.[21] Each domain corresponds to an $\alpha$ relaxation. For strong intra- and intermolecular hydrogen bond domains the $\alpha$ relaxation ($\alpha_1$) occurs at ≈ 300°C, and for weak intra- and intermolecular hydrogen bond domains two $\alpha$ relaxations occur between ≈ 140 and 240°C for $\alpha_{2\text{-}2}$ and between ≈ 215 and 290°C for $\alpha_{2\text{-}1}$ (depending on the measurement methods).[21] Thus, we may attribute the peak of large magnitude observed on the tan $\delta = f(T)$ curves at ≈ 150°C to the $\alpha_{2\text{-}2}$ relaxation process (which is called $\alpha$ for simplicity). By definition, the $\alpha$ relaxation is the viscoelastic evidence of the glass transition and this transition is a cooperative one. If these curves are analyzed in more detail, we observe that the $\alpha$ relaxation for sample a exhibits two distinct peaks at 150°C (temperature taken at the maximum of the peak) and at 175°C. We may conclude that some differences among all the samples exist in the glassy state while only sample a differs from the others at $T > T_\alpha$. All data

**Table II Literature Comparison of Chemical Shifts and Their Assignments for Cellulose and LiCl/DMAc Samples**

| Sample | Solvent | $^{13}$C-NMR Chemical Shifts (ppm) C1 | C2 | C3 | C4 | C5 | C6 | Ref. |
|---|---|---|---|---|---|---|---|---|
| a. Cellulosic samples | | | | | | | | |
| Cellobiose $\alpha$ | — | 92.6 | 72.0 | 72.1 | 79.4 | 70.9 | 60.7 | 15 |
| Cellulose | DMAc/LiCl | 103.9 | 74.9 | 76.6 | 79.8 | 76.6 | 60.6 | 13 |
| Cellulose | NAOH/$D_2O$ | 104.5 | 74.7 | 76.1 | 79.8 | 76.3 | 61.5 | 15 |
| Sample d | DMAc/LiCl | 103.5 | 74.5 | 76.3 | 79.5 | 76.3 | 60.5 | This work |
| Samples b & c | DMAc/LiCl | 103.5 | 74.5 | 76.3 | 79.5 | 76.3 | 60.5 | This work |
| b. Solvent systems | | | C′1 | C′2 | C′3 | C′4 | | |
| DMAc/LiCl | — | | 171.7 | 39.3 | 35.3 | 22.2 | | 15 |
| DMAc/LiCl | — | | 171 | 38.3 | 35.1 | 21.7 | | This work |
| c. Melamine formaldehyde resin | | | | | | | | |
| Triazine rings | — | | Unsubstituted 167<br>Monosubstituted 166<br>Disubstituted 165 | | | | | |
| —N($CH_2$)$\underline{C}H_2OCH_2NH$ | — | | 72 | | | | | 26 |
| —N($CH_2$)$\underline{C}H_2OH$ | — | | 71 | | | | | |
| —NH$\underline{C}H_2OCH_2NH$— | — | | 68 | | | | | |
| —NH$\underline{C}H_2OH$ | — | | 65 | | | | | |
| —N($CH_2$)$\underline{C}H_2N(CH_2)$ | — | | 61 | | | | | |
| —N($CH_2$)$\underline{C}H_2NH$— | — | | 53 | | | | | |
| —NH$\underline{C}H_2NH$— | — | | 47 | | | | | |

from these measurements are presented in Table III.

For a $T_c$ of 140°C and for the variations of the storage modulus with the temperature (Fig. 9), the same relaxations as those observed previously for a $T_c$ of 85°C are obtained; but for the $\alpha$ relaxation the characteristic temperatures are differ-

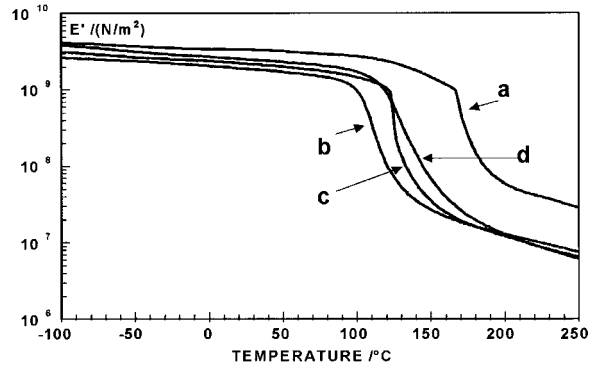


**Figure 7** Variations of the storage modulus $E'$ versus temperature ($T_{cure}$ = 85°C for 3 h) for composite materials a–c obtained at pH 6, 7, and 9 and cellulosic material d.

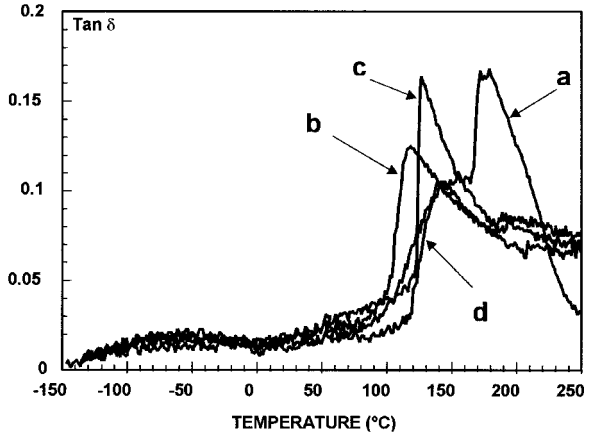


**Figure 8** Variations of tan $\delta$ versus temperature ($T_{cure}$ = 85°C for 3 h) for composite materials a–c obtained at pH 6, 7, and 9 and cellulosic material d.

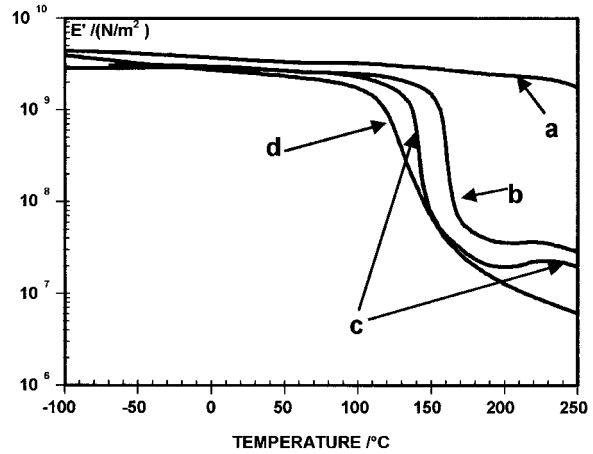


**Figure 9** Variations of the storage modulus a–c $E'$ versus temperature ($T_{cure}$ = 140°C for 3 h) for composite materials a–c obtained at pH 6, 7, and 9 and cellulosic material d.

ent for each sample. Differences between the four samples clearly appear for $T > T_\alpha$. For sample a the decrease of the storage modulus is not observed for temperatures up to 250°C. For samples b and c the storage modulus increases for $T > T_\alpha$ and reaches a maximum for temperatures close to 230°C. The last point that we may notice is the differences in the magnitude of the storage modulus variations at the $\alpha$ transition. For the variations of tan $\delta$ with the temperature (Fig. 10), the $\beta$ relaxation is observed for all the samples in the same temperature range and with the same magnitude. No difference for the $\beta$ relaxation between samples cured at 85 and 140°C exists. A peak of very small magnitude is observed at 180°C for sample a. For samples b and c the magnitude of the $\alpha$ relaxation is practically the same and is higher than observed for samples cured at 85°C; only the characteristic temperatures are different: $T_\alpha$ = 165 and 160°C for samples b and c, respectively.

Moisture sorption experiments were carried out for the various RH conditions defined above. Measurements of moisture content $w$ (grams of moisture regained per 100 g of dry polymer) of samples were made as a function of time $t$. Figure 11 shows the results obtained; we observe that all studied samples exhibit the characteristic sigmoidal shape. For each RH the regain of water increases roughly to reach a maximum value ($w_\infty$) at the steady state (at an infinite time). We observe that this value $w_\infty$ (reported in Table IV) increases rapidly with the RH value.

## DISCUSSION

$^{13}$C-NMR spectroscopy was widely used to characterize the chemical structures of different modified melamine formaldehyde resins,[22–25] but only recent works such as those of Mercer and Pizzi[26,27] are devoted to the characterization of resin/cellulose mixtures. These authors focused their works on melamine formaldehyde/wood particleboard and melamine-urea-formaldehyde/wood particleboard. That work shows the characteristic chemical shifts and their assignments for the melamine formaldehyde resin. They are also reported in Table II. The comparison of our data and those obtained by Mercer and Pizzi[26] shows that the peaks at 164.9 and 168.2 ppm observed in Figure 6 for sample c can be attributed to the presence of the resin. Nevertheless, the magnitude of these peaks is very small and a quantitative analysis seems rather risky. In other words, the amount of condensed or cocondensed resin, which remains in sample c after washing, is very small. These peaks are not observed for sample b (Fig. 5). This lack of peaks indicates that no resin remains in the product after washing the resin/cellulose system. Thus, we may conclude that, after a cure performed at 85°C for 3 h, and for samples obtained from aqueous solution at pH 7 and 9, the resin is practically uncondensed and/or not cocondensed with the cellulose. Consequently, there are mainly hydrolysis reactions that are involved with these experimental conditions. On the other hand, the lack of a $^{13}$C-NMR spectrum for sample a cured at 85°C and for all the samples

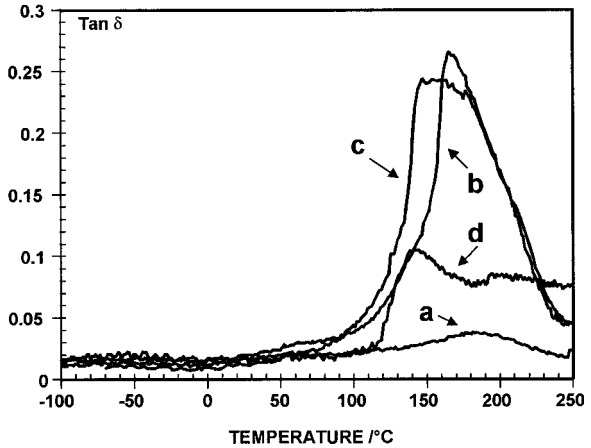


**Figure 10** Variations of tan $\delta$ versus temperature ($T_{cure}$ = 85°C for 3 h) for composite materials a–c obtained at pH 6, 7, and 9 and cellulosic material d.

**Table III Dynamic Mechanical Analysis Data Collected from Experiments Performed on Samples a–d**

| $T_{cure}$ (°C) | Sample | $E'$ (−100°C) ($\times 10^9$ N m$^{-2}$) | $E'$ (+200°C) ($\times 10^7$ N m$^{-2}$) | $(\tan \delta)_{max}$ | $T_\alpha$ (°C) |
|---|---|---|---|---|---|
| 85 | a | 4.1 | 6.0 | 0.1–0.162 | 150–175 |
| | b | 2.8 | 1.4 | 0.125 | 115 |
| | c | 3.0 | 1.4 | 0.160 | 125 |
| | d | 4.0 | 1.4 | 0.1 | 140 |
| 140 | a | 4.2 | 220 | 0.04 | — |
| | b | 2.9 | 4.0 | 0.23 | 165 |
| | c | 3.0 | 1.9 | 0.22 | 155 |
| | d | 4.0 | 1.05 | 0.1 | 140 |

Samples a–c are composites obtained at pH 6, 7, and 9, respectively, and d is a cellulosic material.

cured at 140°C, which is due to its inability to dissolve the composite, shows that the degree of transformation is so significant that the final product exhibits a high resistance to the solvents. Nevertheless, at this stage of the work it is not possible to know the nature of the chemical reactions engaged.

The curves obtained from the viscoelasticity measurements show the variations of the storage modulus and the loss tangent lead to the conclusion that no difference between the sample a cellulose and samples b and c cured at 85°C exists. This means that the resin does not influence the viscoelastic properties of the cellulose. Keeping in mind the $^{13}$C-NMR results, it is clear that neither self-condensation of the resin nor cocondensation reactions of the resin with the cellulose occur with these experimental conditions. On the other hand, from a structural point of view, the cellulose must be considered as a porous semicrystalline polymer. Absorption of water concerns the vitreous phase of the sample, because this phase exhibits a larger free volume than the crystalline one. This leads to an inflation of the amorphous domains and a decrease of the intra- and intermolecular hydrogen bonds that exist at the border between the amorphous and the crystalline domains. As a consequence, water molecules create enough disorder to transform a part of the crystalline phase into a vitreous one. This phenomenon is generally reversible; for instance, heating the cellulose in such a way that water is evaporated leads to an increase of the rate of crystallinity of the cellulose.[28–30] Thus, the small variations of $T_\alpha$ observed for samples b and c on the loss tangent curve (Fig. 8) can be attributed to a small change of the intra- and intermolecular hydrogen bonds in the vitreous phase.

On the other hand, according to the works of Hill and Kozlowski,[31] dynamic mechanical analysis can be used as a powerful tool to determine the crosslinking density of cured melamine formaldehyde resins mixed with a polyol. They showed that, depending on the resin/polyol ratio, important changes appear in the values of the storage modulus in the rubberlike state and in the tan δ

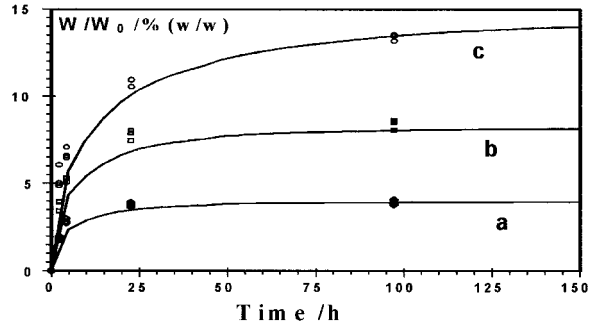


**Figure 11** Variations of $W/W_0$ versus time performed on recycled cellulosic sample e and for relative humidities of 25% (curve a), 73% (curve b), and 95% (curve c). ($W_0$ is the initial weight of samples.)

**Table IV Values of Moisture Content at Equilibrium ($w_\infty$) Obtained for Samples e and f**

| | $w_\infty$/(g $H_2O$/100 g) | | |
|---|---|---|---|
| Sample | 25% RH | 73% RH | 95% RH |
| e | 4.1 | 8.8 | 14.4 |
| f | 2.95 | 7.4 | 13.4 |

Samples e and f are a cellulosic sample and a resin/recycled cellulosic composite, respectively.

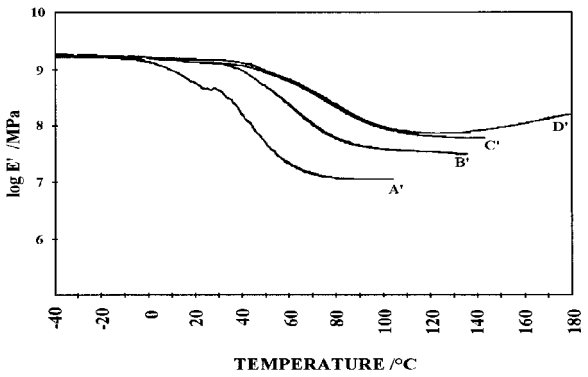


**Figure 12** The storage modulus of the dynamic properties of films of composite materials of acrylic polyol (AC) and melamine formaldehyde resin (MF). The AC/MF ratios (% w/w) are 92 : 8 (curve A′), 88 : 12 (curve B′), 84 : 16 (curve C′), and 60 : 40 (curve D′).

plots. Using the theory of network formation,[32] which predicts that the degree of cocondensation reactions is the highest for the stoichiometric ratio of reactants, and the theory of rubber elasticity, which predicts that the value of the storage modulus is directly proportional to the crosslinking density,[32,33] these authors found that, depending on the resin/polyol ratio, we may distinguish three kinds of curves. Figure 12 shows these three situations schematically. If the resin content is lower than the stoichiometric one (Fig. 12, curves A′ and B′), the value of the storage modulus in the rubberlike state is low but increases as the amount of resin increases. It follows for the loss tangent curve that a shift toward the highest temperatures of the peak characterizes the $\alpha$ relaxation. This is observed for sample a cured at 85°C (Figs. 7, 8). If the resin content corresponds to the stoichiometric one, the value of the storage modulus must reach a maximum (Fig. 12, curve C′). Finally, if the resin content is higher than the stoichiometric one (Fig. 12, curve D′), the variations of the storage modulus at $T > T_\alpha$ exhibits a small peak that is due to the self-condensation reactions of the resin in excess. This is observed for samples b and c cured at 140°C (Fig. 9). For sample a cured at 140°C the variations of the storage modulus for $T > T_\alpha$ follow any of the behaviors expected for a cocondensation mechanism, but the values obtained show that the transformation exists.

To summarize the mechanical properties, all these results show that under acid conditions, whatever the temperature of cure, mainly self-condensation reactions of the resin appear. Under basic or neutral conditions and low curing temperature mainly hydrolysis reactions occur whereas at high temperatures mainly cocondensations of the resin with the cellulose occur.

The moisture sorption kinetics agree well with a Fickian diffusion law as shown in Figure 13 for which sorption data are plotted as $w/w_\infty$ versus the square root of the dimensionless parameter $t/l^2$; $w_\infty$ is the moisture content at equilibrium, $D$ is the water apparent diffusion coefficient, and $l$ is the film thickness.

By adjusting the values of $D$, the water apparent diffusion coefficients are $10^{-6}$ and $4 \times 10^{-7}$ $cm^2\ s^{-1}$ for sample e and sample f, respectively. The set of experimental data is fairly described by theoretical curves calculated from Crank[34]:

$$\frac{w}{w_\infty} = 4\left(\frac{\tau}{\pi}\right)^{1/2} \quad \text{for} \quad \tau \geq 0.0492 \tag{1}$$

$$\frac{w}{w_\infty} = 1 - \frac{8}{\pi^2}\sum_0^\infty \frac{1}{(2n+1)^2}\exp[-(2n+1)^2\pi^2\tau] \quad \text{for} \quad \tau \geq 0.0492 \tag{2}$$

where $\tau = Dt/l^2$.

The $D$ values obtained in this work are in good agreement with those obtained for different cellulosic samples or cellulosic composite materials (see Table V). On the other hand, the variations of $w_\infty$ with the RH lead to the experimental sorption isotherm presented in Figure 14 for a pure cellulosic sample and for a resin/cellulose composite material. On this curve we may distinguish for a pure cellulosic sample three ranges of RH values

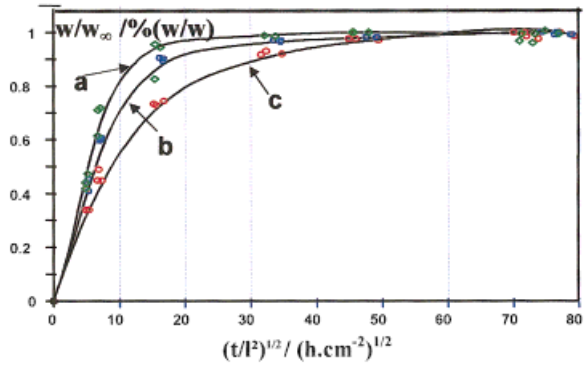


**Figure 13** The water sorption kinetics of recycled cellulosic sample e with the sorption rate ($W/W_\infty$) as a function of the dimensionless parameter $(t/l^2)^{1/2}$ with RHs of 25% (curve a), 73% (curve b), and 95% (curve c).

**Table V Values of Diffusion Coefficient of Water Through Cellulosic and Composite Materials**

| Sample | Author | $T$ (°C) | RH (%) | Diffusion Coefficient ($cm^2\ s^{-1}$) | Ref. |
|---|---|---|---|---|---|
| Regenerated cellulose | Hauser and Mc Laren | 25 | 20 | $< 10^{-9}$ | 38 |
| Ethyl cellulose | Wellons and Stannett | 25 | 21–84 | $180 \times 10^{-6}$ | 39 |
| Melamine formaldehyde resin | Smith and Fisher | 100 | 100 | $1.97 \times 10^{-7}$ | 40 |
| Poly(ethylene terephthalate) | Langevin et al. | 25 | 20.5–59 | $4.5 \times 10^{-9}$ | 41 |
| Cellulose acetate | Thomas | 30 | 50 | $1.7 \times 10^{-9}$ | 42 |
| Sample e (recycled cellulose) | Devallencourt et al. | 25 | 25–95 | $10 \times 10^{-7}$ | This work |
| Sample f (composite material) | Devallencourt et al. | 25 | 25–95 | $4 \times 10^{-7}$ | This work |

for which the variations of $w_\infty$ with RH are different. Up to about 20% RH we observe a drastic increase of $w_\infty$; from 20% < RH < 70% the $w_\infty$ varies linearly with RH and for 70% < RH the $w_\infty$ increases drastically with the RH. These variations are expected for a cellulosic material[22] and are characteristic of the water sorption by a porous material. Up to 70% RH the water sorption is described by a modified dual mode sorption.[33–36] This model postulates that a gas dissolved in a glassy polymer consists of the following two distinct molecular populations.

1. molecules dissolved in a limited number of fixed, preexisting microcavities or at fixed sites in the polymer matrix. The concentration of molecules dissolved in microcavities is related to the penetrant equilibrium pressure by the Langmuir mode (Fig. 15) and can engage hydrogen bonds with the polar group of the cellulose.
2. molecules dissolved in the polymer by an ordinary diffusion process. This is the classic Henry law that characterizes the water sorption for a dense polymer (Fig. 15).

For >70% RH we have now to take into account a modified Henry law, the Flory–Huggins law, which indicates that water forms local clusters leading to a sweeping effect.

The main difference that appears between a pure cellulosic sample and a resin/cellulose sample appears at low RH values. Thus, mainly the Langmuir mode is modified by the presence of the resin and the variations tend toward what it is expected for a dense polymer: the resin is mainly located in the cavities.

From these observations we may now propose a complete scenario of the different phenomena (reactions) that occur when a cellulosic sample is

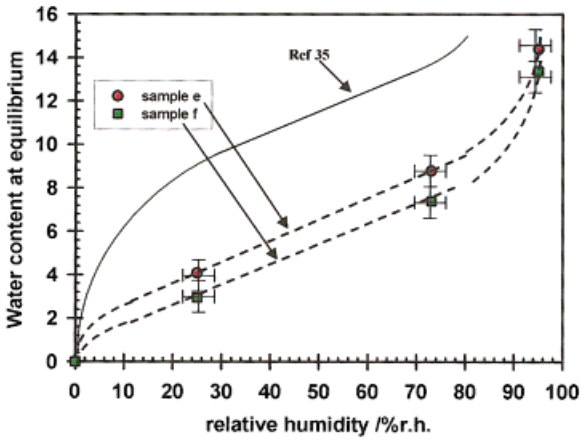


**Figure 14** The experimental isotherm curves of water sorption obtained on recycled cellulosic sample e and resin/recycled cellulosic composite sample f. The composites were obtained at pH 7 and a $T_{cure}$ of 100°C for 3 h. Reference 35 concerns a cellulosic sample with an 85% vitreous phase.

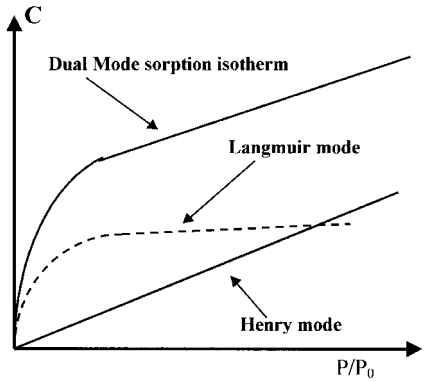


**Figure 15** Typical dual mode sorption isotherms and their components, where the $P/P_0$ ratio indicates the activity of the penetrant molecules.

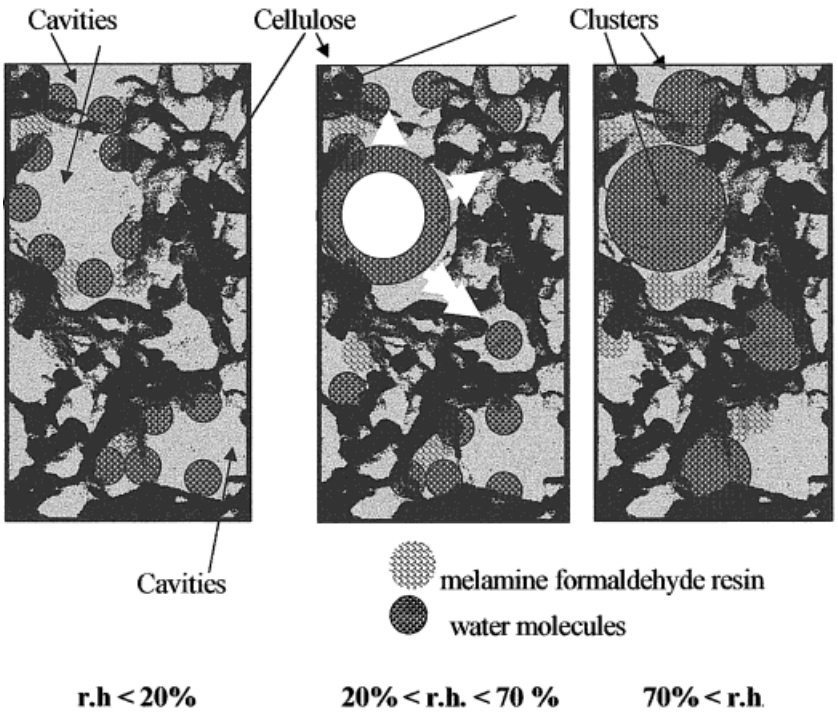


**Figure 16** A schematic explanation of the mechanisms occurring during the sorption of the water/resin in the cellulosic material and during the cure processing.

immersed in aqueous solutions of melamine formaldehyde resin (pH 7) cured at 100°C (Fig. 16). First, when water is adsorbed by a cellulose, water molecules, which act as a vector for the resin, swept the resin that will stay in the microcavities. Then, depending on the cure temperatures and the pH values, hydrolysis, self-condensation, or cocondensation reactions will occur. For greater RH values, only water molecules will practically diffuse through the dense cellulosic part of the matrix. This is confirmed by the fact that the same modified Henry law describes the variations of $w_\infty$ with RH for a pure or modified cellulosic sample and also by the fact that the same Flory–Huggins law describes the behavior for a pure or a modified cellulosic sample at a high RH. Finally, the formation of clusters at high RH values remains valid even for resin/cellulosic composite materials.

## CONCLUSION

The introduction of a melamine formaldehyde resin in a cellulosic matrix causes different reactions, depending on the value of the pH and the cure temperature. We show that mainly self-condensation reactions of the resin occur for $T_{\text{cure}} = 140$°C and pH 6. Mainly cocondensation reactions occur for same cure temperature and pH $\geq 7$. Mainly hydrolysis reactions exist for $T \leq 80$°C.

The study of the moisture sorption by the composite material elaborated at pH 7 and a cure temperature of 100°C shows the presence of a dual mode sorption (the Langmuir and the Flory–Huggins modes) that depends upon the RH. The main difference between a pure cellulosic sample and a composite material appears at low RH values in the Langmuir mode and confirms that melamine formaldehyde resin is mainly located in the microcavities of the cellulosic matrix.

## REFERENCES

1. Brainbridge, R. Sail 1977, 8, 142.
2. Kay, M.; Price, A. F.; Lavery, I. J Fire Retardant Chem 1979, 6, 69.
3. Jones, F. N.; Chu, G.; Samaraweera, U. Prog Org Coat 1994, 24, 189.
4. Samaraweera, U.; Jones, F. N. J Coat Technol 1992, 64, 69.
5. Blank, W. J. J Coat Technol 1982, 54, 26.

6. Blank, W. J.; Hensley, W. L. J Paint Technol 1974, 46, 46.
7. Blank, W. J. J Coat Technol 1979, 51, 61.
8. Blank, W. J.; Koral, J. N.; Petropoulos, J. C. J Paint Technol 1970, 42, 609.
9. Bauer, D. R. Prog Org Coat 1986, 14, 133.
10. Koral, J. N.; Petropoulos, J. C. J Paint Technol 1966, 38, 600.
11. Devallencourt, C.; Saiter, J. M.; Fafet, A.; Ubrich, E. Thermochim Acta 1995, 259, 143.
12. Devallencourt, C.; Saiter, J. M.; Capitaine, D. Polym Degrad Stabil 1996, 52, 327.
13. Devallencourt, C.; Saiter, J. M.; Capitaine, D. Polym Eng Sci 1999, 39, 413.
14. McCormick, C. L.; Callais, P. A.; Hutchinson, B. H. Macromolecules 1985, 18, 2394.
15. Nehls, I.; Wagenknecht, W.; Philipp, B.; Stscherbina, D. Prog Polym Sci 1994, 19, 29.
16. Bradley, S. A.; Carr, S. H. J Polym Sci Polym Phys Ed 1976, 14, 111.
17. Kimura, M.; Nakano, J. J Polym Sci Polym Lett Ed 1976, 14, 741.
18. Pankonin, B.; Habeger, C. J Polym Sci Part B Polym Phys 1988, 26, 339.
19. Stratton, R. A. J Polym Sci Polym Chem Ed 1973, 11, 535.
20. Dollimore, D.; Hoath, J. M. Thermochim Acta 1981, 45, 87.
21. Manabe, S. I.; Iwata, M.; Kamide, K. Polym J 1986, 18, 1.
22. Pash, H.; Hovakeemian, G.; Lahalih, S. J Polym Sci Part A Polym Chem 1991, 29, 525.
23. Ebdon, J. R.; Hunt, B. J.; O'Rourke, W. T. S. Br Polym J 1987, 19, 197.
24. Dawbarn, M.; Ebdon, J. R.; Hewitt, S. J.; Hunt, J. E. B.; Williams, I. E.; Westwood, A. R. Polymer 1978, 19, 1309.
25. Ebdon, J. R.; Heaton, P. E. Polymer 1977, 18, 971.
26. Mercer, A. T.; Pizzi, A. J Appl Polym Sci 1996, 61, 1697.
27. Mercer, A. T.; Pizzi, A. J Appl Polym Sci 1996, 61, 1687.
28. Hatakeyama, T.; Hatakeyama, H.; Ikeda, Y. Macromol Chem 1987, 18, 1875.
29. Yano, S.; Hatakeyama, H. Polymer 1988, 29, 566.
30. Kimura, M.; Hatakeyama, T.; Nabano, J. J Appl Polym Sci 1974, 19, 3069.
31. Hill, L. W.; Kozlowski, K. J Coat Technol 1987, 59, 63.
32. Miller, D. R.; Macosko, C. W. Macromolecules 1976, 9, 206.
33. Harrison, D. J. P.; Yates, W. R.; Johnson, J. F. Rev Macromol Chem Phys 1985, 4, 481.
34. Crank, J. The Mathematics of Diffusion, 2nd ed.; Clarendon Press: Oxford, U.K., 1975.
35. Berthold, J.; Desbrieres, J.; Rinaudo, M.; Salmen, L. Polymer 1994, 35, 5729.
36. Koros, W. J.; Chern, R. T. In Handbook of Separation Process Technology; Rousseau, R. W., Ed.; Wiley–Interscience: New York, 1987; p 862–953.
37. Vieth, W. R. Membrane System, Analysis and Design; Hanser: New York, 1988; p 9–12.
38. Hauser, P. M.; Mc Laren, A. D. Ind Eng Chem Ind Ed 1948, 40, 112.
39. Wellons, J. D.; Stannett, V. J Polym Sci A1 1966, 4, 593.
40. Smith, P. M.; Fisher, M. M. Polymer 1984, 25, 84.
41. Langevin, D.; Grenet, J.; Saiter, J. M. Eur Polym J 1993, 30, 339.
42. Thomas, A. M. J Appl Chem 1951, 1, 141.